Journal of Alloys and Compounds 509 (2011) 2461–2465

Contents lists available at ScienceDirect

Journal of Alloys and Compounds

journal homepage: www.elsevier.com/locate/jallcom

Investigation of structural, morphological and optical properties of nickel zinc oxide films prepared by sol–gel method

D. Duygu Dogan, Yasemin Caglar*, Saliha Ilican, Mujdat Caglar

Department of Physics, Anadolu University, Eskisehir 26470, Turkey

ARTICLE INFO

Article history:
Received 1 October 2010
Accepted 7 November 2010
Available online 18 November 2010

Keywords:
NiZnO
Sol–gel process
Crystalline structure
Absorption edge

ABSTRACT

NiZnO films have been prepared on glass substrates by sol–gel spin coating method. Nickel (II) nitrate hexahyrate and zinc acetate dihydrate were used as precursors. Surface morphology and crystalline structure of the films were investigated by field emission scanning electron microscopy (FESEM) and X-ray diffractometer, respectively. X-ray diffraction (XRD) patterns showed that the films are polycrystalline nature. It was observed that crystal structure changed from wurtzite (ZnO) to cubic (NiO) structure. The lattice constants crystallite size and preferred orientation were calculated from XRD data. The surface morphology of the films changed with Ni concentration. The average transmittance of the ZnO film decreased from 84% to 58% in the visible region. The absorption edge varied from 3.26 to 3.89 eV with increasing Ni concentration.

1. Introduction

Zinc oxide (ZnO) films have been widely studied because of their specific electrical, optical and mechanical properties, low material cost and low deposition temperature. They can be used in optoelectronic devices and it is useful material for the optoelectronic devices as transparent conducting oxide (TCO) [1]. Also, recently there is growing interest in nickel oxide (NiO), which is a metal oxide material, because of its applications in many areas. Catalytic, magnetic, electrochromotic, optical and electrochemical properties are that some great feature of NiO [2]. In the literature, the optical band gaps of bulk NiO and bulk ZnO are 4.00 eV and 3.37 eV, respectively [3–5]. Furthermore NiO films are suitable for magnetoresistance sensors, chemical sensors [6,7], electrochromic devices [8] and transparent p-type semiconducting layer, smart windows [9] and dye sensitized photocathodes [10–12]. Some methods can be used for the preparation of NiZnO films such as sputtering [13], evaporation [14], electrodeposition [15], thermal decomposition [16], pulse laser deposition (PLD) [17–19], spray pyrolysis [20], and sol–gel techniques [21]. Among these methods, the sol–gel method is an attractive one due to its simplicity, safety, non-vacuum system of deposition, and inexpensive. Other advantages of this method are that it can be adapted easily for production of large-area films, and to get varying band gap materials during the deposition process.

Although pure ZnO and NiO films have been studied by many research groups, the NiZnO films have been rarely studied. Also in these works about NiZnO, in general, small amounts of Ni were incorporated to ZnO in the $Ni_xZn_{1-x}O$ structure and the physical properties of these films were investigated depending on the small x values [22,23]. In the $Ni_xZn_{1-x}O$ structure, while x value varies from 0 to 1, it is observed ZnO, NiO and related complex structures depending on the x value. The crystal structure changes from wurtzite (ZnO) to cubic (NiO) structure. So, the determination of the physical properties of the structural phase transition between two different structures can be very useful. In our previous works, the some physical properties of similar structures such as MgZnO and CdZnO were reported [24–26].

Although ZnO and NiO films produced by the sol–gel spin coating method have been reported by many research groups, NiZnO films have seldom been studied. According to our knowledge, there are a little detailed works on NiZnO films obtained by the sol–gel spin coating method [15,24]. In this work, NiZnO films were prepared by sol–gel spin coating method. The structural, morphological and optical properties of these films prepared at different solution ratios to get the transition from ZnO to NiO structure were studied.

2. Experimental

A set of NiZnO films was prepared by sol–gel process using a spin coating technique onto glass substrates. The glass substrates were first cleaned by detergent, and then in methanol and acetone each for 10 min. At last, the substrates were rinsed with deionized water and dried with nitrogen. To obtain the sol, the precursor zinc acetate dihydrate ($Zn(CH_3COO)_2{\cdot}H_2O$, ZnAc) and nickel (II) nitrate hexahydrate

* Corresponding author. Tel.: +90 222 3350580; fax: +90 222 3204910.
E-mail addresses: yasemincaglar@anadolu.edu.tr, ycaglar@semiconductorslab.com (Y. Caglar).

0925-8388/$ – see front matter © 2010 Elsevier B.V. All rights reserved.
doi:10.1016/j.jallcom.2010.11.054

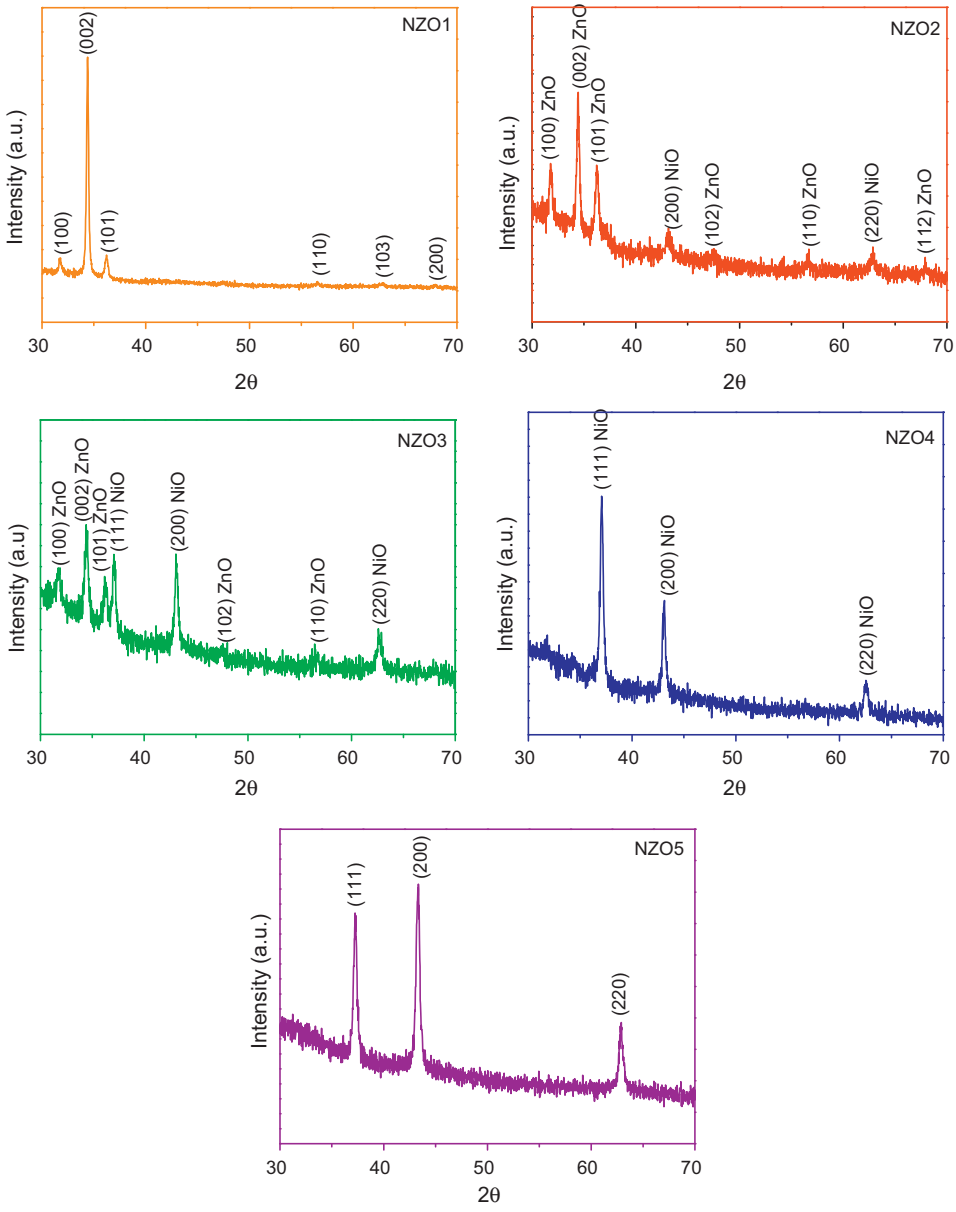

Fig. 1. XRD patterns of the NiZnO films.

($Ni(NO_3)_2{\cdot}6H_2O$, NiN) were first dissolved into 2-methoxyethanol ($C_3H_8O_2$) as a solvent and by adding monoethanolamine (C_2H_7NO,·MEA), which acts as the stabilizer. Molar ratio of MEA to ZnAc or NiN was maintained at 1:1. ZnAc and NiN of 0.5 M were mixed together in different nominal solution volume ratios to obtain ZnO, Ni(0.25)Zn(0.75)O, Ni(0.50)Zn(0.50)O, Ni(0.75)Zn(0.25)O, NiO films (named as NZO1, NZO2, NZO3, NZO4, NZO5, respectively). The solutions were stirred at 60 °C. The substrates were placed on the sample holder and were rotated at a speed of 3000 revolutions per min (rpm) for 30 s. Immediate drying after successive coating was done at 300 °C for 10 min. This process was repeated ten times. The films were finally annealed at 500 °C for 1 h in air for crystallization and phase formation. The obtained films have different colours, varying between colourless (transparent) for the ZnO to brown for the NiO.

XRD experiments were performed in air with X-ray powder diffractometer (BRUKER D8 Advance). The diffractometer reflection of all the films was taken at room temperature. The films were mounted on rotating sample holders. A sealed X-ray tube operated at 40 kV and 40 mA with CuKα radiation was used. All measurements were performed in reflection geometry as coupled θ–2θ scans ($30^\circ \leq 2\theta \leq 70^\circ$) at a divergent slit of 0.5 mm width. Surface morphology was studied using Zeiss Ultraplus FESEM. Optical transmittance measurements of the films were carried out by double beam Shimadzu UV 2450 spectrometer with an integrating sphere in the wavelength range 190–900 nm.

3. Results and discussions

The XRD patterns of the NiZnO films have been realized in order to evaluate crystalline phase and crystallite orientation. Fig. 1 shows the XRD patterns of these films. The observed indexed peaks in these XRD patterns are fully matched with the corresponding hexagonal wurtzite structure ZnO (zincite, PDF number: 036-1451 [27]) and cubic structure NiO (bunsenite, PDF number: 047-1049 [28]). The XRD results indicate that all the films have the polycrystalline structure. As seen in Fig. 1, the NZO1 film has highly oriented (0 0 2) peak. The other peaks in this film are corresponds to the (1 0 0) and (1 0 1) peaks of the hexagonal wurtzite structure. As seen from Fig. 1, 2θ values of (0 0 2) peaks of NZO1, NZO2 and NZO3 films increased with increasing nickel concentration. With the increasing nickel concentration, it is clearly observed that the peak intensities of ZnO structure decrease and new peaks which belong to NiO structure begin to appear. In the NZO3 film, the

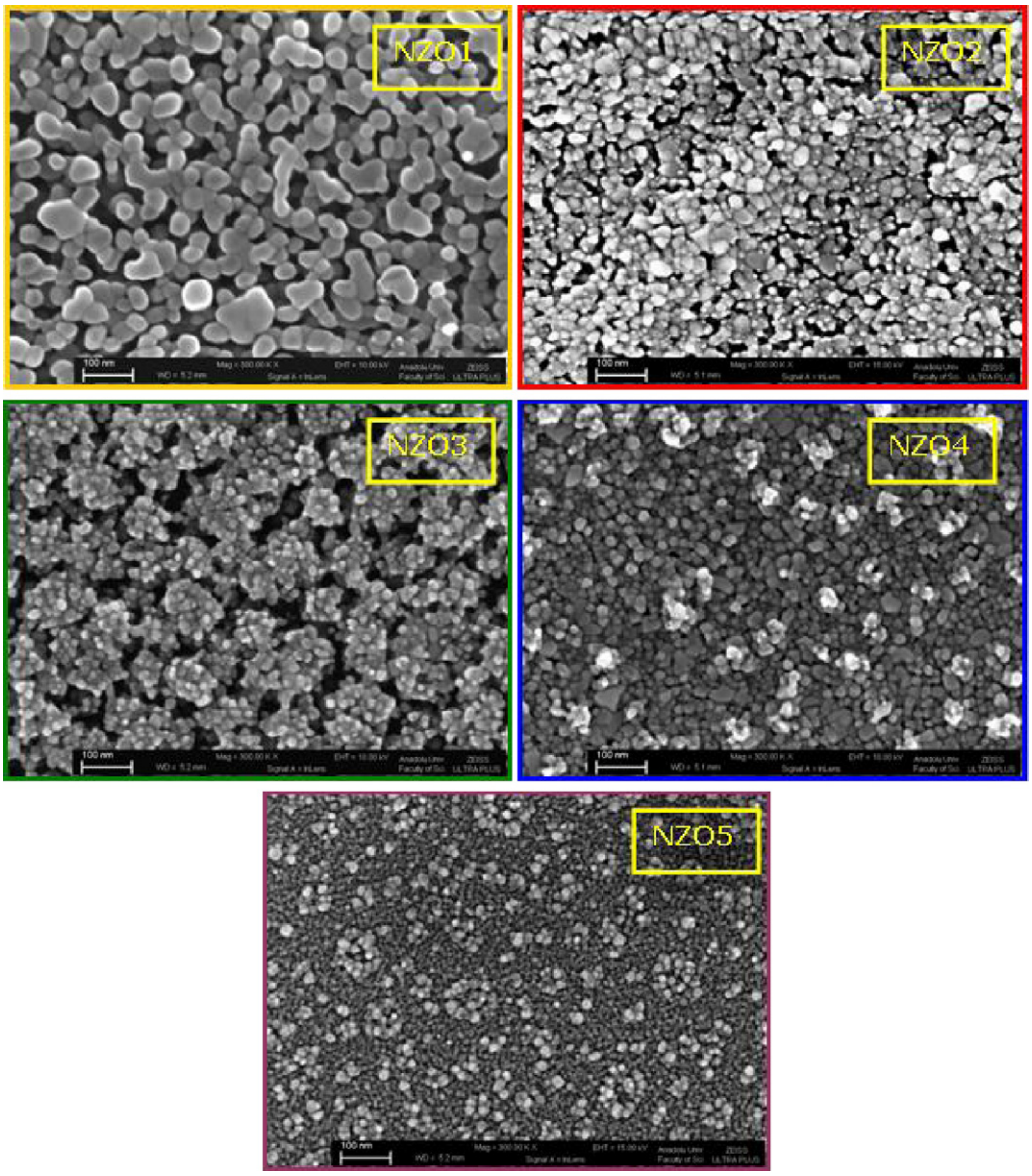

Fig. 2. FESEM images of the NiZnO films.

peaks belong to both ZnO and NiO structures are shown. That is, this complex structure includes both hexagonal and cubic structures. It is very interesting to note that the peaks belong to ZnO are not observed in the NZO4 film although NiO peaks are little seen in the NZO2 film. NZO5 film has an oriented (2 0 0) peak. The other peaks in this film correspond to the (1 1 1) and (2 2 0) peaks of the cubic structure. The miller indices *(hkl)*, 2θ, *d* values of the all films are given in Table 1.

The crystallite size of the NiZnO films was calculated by using the well-known Scherrer's equation [29]

$$D = \frac{k\lambda}{\beta \cos \theta} \quad (1)$$

where k is a constant (0.9), λ is the wavelength of X-rays, β is the full width-at-half-maximum (FWHM) and θ is the angle of diffraction. The crystallite size was calculated by resolving the highest intensity peak belonging to the single phase. There are mixture phases in some films. Therefore, the crystallite size values were evaluated according to the highest peaks belonging to the ZnO and the NiO phases in the NZO2 and NZO3 films. The crystallite sizes and β values of the films are given in Table 1. As seen in this table,

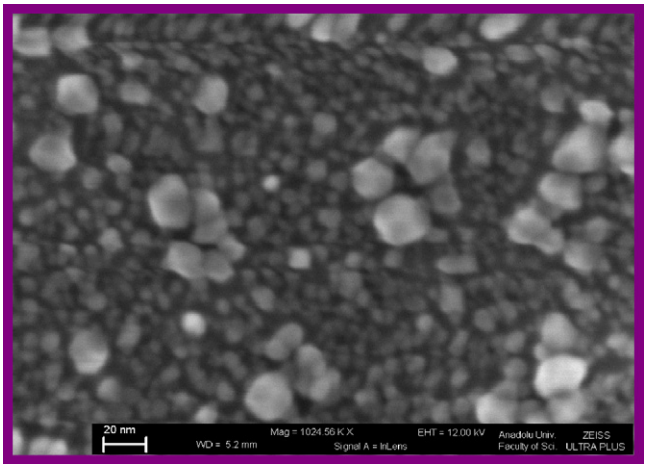

Fig. 3. FESEM image of NZO5 film at 1×10^6 magnifications.

Table 1
Structural parameters of the NiZnO films.

Film	*hkl*	2θ	*d* (Å)	β	*D* (nm)
NZO1	ZnO (1 0 0)	31.731	2.81771	–	–
	ZnO (0 0 2)	34.395	2.60530	0.222	37
	ZnO (1 0 1)	36.214	2.47853	–	–
	ZnO (1 1 0)	56.546	1.62623	–	–
	ZnO (1 0 3)	62.856	1.47729	–	–
	ZnO (2 0 0)	67.934	1.37870	–	–
NZO2	ZnO (1 0 0)	31.781	2.81341	–	–
	ZnO (0 0 2)	34.440	2.60201	0.288	29
	ZnO (1 0 1)	36.266	2.47510	–	–
	NiO (2 0 0)	43.075	2.09827	0.302	31
	ZnO (1 0 2)	47.618	1.35029	–	–
	ZnO (1 1 0)	56.618	1.62434	–	–
	NiO (2 2 0)	62.874	1.47690	–	–
	ZnO (1 1 2)	67.927	1.37882	–	–
NZO3	ZnO (1 0 0)	31.782	2.81329	–	–
	ZnO (0 0 2)	34.460	2.60053	0.305	27
	ZnO (1 0 1)	36.241	2.47675	–	–
	NiO (1 1 1)	37.106	2.42097	0.305	27
	NiO (2 0 0)	43.111	2.09662	–	–
	ZnO (1 0 2)	47.501	1.35342	–	–
	ZnO (1 1 0)	56.763	1.62052	–	–
	NiO (2 2 0)	62.854	1.47734	–	–
NZO4	NiO (1 1 1)	37.084	2.42231	0.327	25
	NiO (2 0 0)	43.077	2.09817	–	–
	NiO (2 2 0)	62.569	1.48339	–	–
NZO5	NiO (1 1 1)	37.261	2.41123	–	–
	NiO (2 0 0)	43.308	2.08754	0.405	21
	NiO (2 2 0)	62.868	1.47705	–	–

the crystallite sizes decrease with increasing nickel molar concentration and the largest crystallite size is observed in NZO1 film. The ionic radius of Ni^{2+} (0.69 Å) is smaller than Zn^{2+} (0.74 Å) [30], therefore, the substitution of Ni by Zn may reduce the crystallite size.

The lattice parameters (a_{hex} and c_{hex}) for hexagonal structure were calculated using Eq. (2) for the NZO1, NZO2, and NZO3 films [29]:

$$\frac{1}{d^2} = \frac{4}{3}\left(\frac{h^2 + hk + k^2}{a_{hex}^2}\right) + \frac{l^2}{c_{hex}^2} \quad (2)$$

The calculated a_{hex} and c_{hex} values are given in Table 2. Lattice parameter (a_{cub}) for cubic structure calculated using Eq. (3) for NZO2, NZO3, NZO4 and NZO5 films [29]:

$$d = \frac{a_{cub}}{\sqrt{h^2 + k^2 + l^2}} \quad (3)$$

The calculated a_{cub} values are also given in Table 2. The lattice parameters of the ZnO film were slightly decreased with increasing Ni concentration. This decrease in the lattice parameters can be expected when Zn^{2+} ions are replaced by Ni^{2+} ions because of the smaller radius of Ni^{2+} ions than Zn^{2+} ions. Similar results were reported by Park and Kim [21] and Thota et al. [23].

The surface morphology of NiZnO films has been studied by FESEM. Fig. 2 shows the FESEM micrographs of all the films. As seen from these micrographs, the crystallite size decreases with increasing Ni concentration. This result is in good agreement with

Table 2
Lattice parameters of the NiZnO films.

Film	ZnO (hexagonal)		NiO (cubic)
	a_{hex} (Å)	c_{hex} (Å)	a_{cub} (Å)
NZO1	3.25361	5.21060	–
NZO2	3.24864	5.20402	4.19654
NZO3	3.24851	5.20106	4.19324
NZO4	–	–	4.19556
NZO5	–	–	4.17508

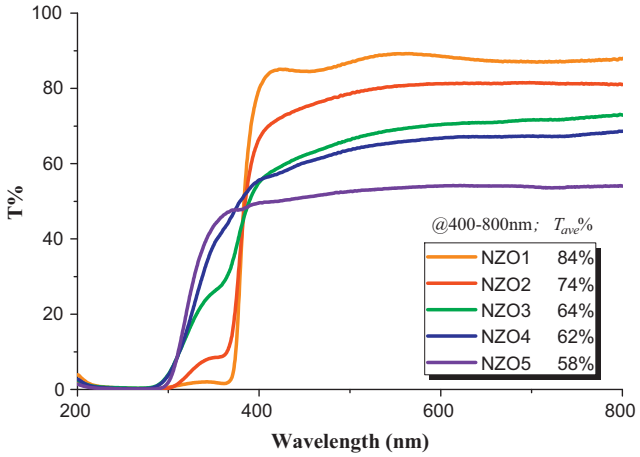

Fig. 4. Optical transmittance spectra of the NiZnO films.

crystallite size values calculated from the XRD results. It is observed that the surface morphology of the films changes depending on the increase in Ni concentration. As the Ni content increases, together with the decrease in the crystallite size was also observed the aggregations on the surface. Although not seen in FESEM images, as the Ni content increases, some fractures were easily seen with the naked eye on the surface. Also, Fig. 3 shows the image of the NZO5 film taken at very high magnification. In this image, cubic structures can be easily seen.

Fig. 4 shows the optical transmittance spectra of the NiZnO films in the range 200–800 nm. The average transmittance values of the films are given in Fig. 4. It was observed that NZO1 film has an average transmittance about 84% in the visible region and the highest average transmittance value belongs to this film. The colour of the films changes from transparent to dark brown with the increasing Ni concentration. So, the average transmittance of the NiZnO film decreases from 84% to 58%. The absorption edge of the films varied from 380 nm to 318 nm.

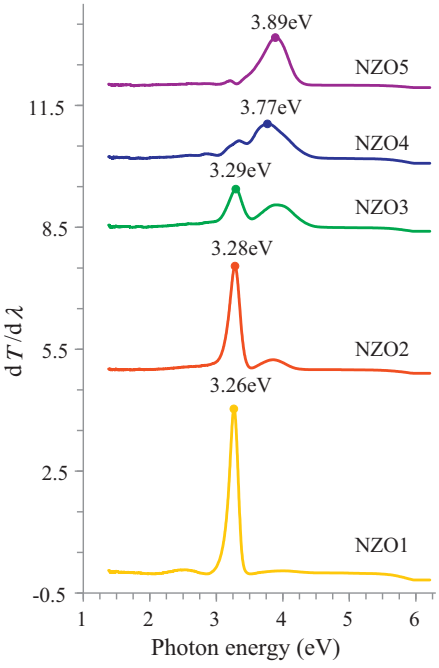

Fig. 5. The plot of $dT/d\lambda$ versus photon energy of the NiZnO films.

To determine the absorption band edge of the NiZnO films, we computed the first derivative of optical transmittance and are presented in Fig. 5. The plots of $dT/d\lambda$ vs. photon energy give the maximum peak position corresponding to the absorption band edge. As seen in Fig. 5, the peak position of the curves shifts to higher energies with Ni concentration. The absorption band values are given in Fig. 5. This suggests that the absorption band edge shifts from 3.26 eV to 3.89 eV with Nickel concentration.

4. Conclusions

The structural, morphological and optical properties of NiZnO films deposited by sol–gel spin coating were investigated. X-ray diffraction spectra indicated that the films are polycrystalline nature. It was also shown from these spectra that the crystallite structure changed from wurtzite to cubic. The structural parameters of the films were determined by using XRD data. The surface morphology was investigated by FESEM. The crystallite size values of the NiZnO films varied from 37 to 21 nm with increasing Ni concentration in solution. This decrease in the grain size was also observed in the FESEM images. The absorption band edge of the films shifted from 3.26 to 3.89 eV with increasing Ni concentration in solution.

Acknowledgements

This work was supported by Anadolu University Commission of Scientific Research Projects under grant no. 061039 and 081029.

References

[1] S. Ghosh, P. Srivastava, B. Pandey, M. Saurav, P. Bharadwaj, D.K. Avasthi, D. Kabiraj, S.M. Shivaprasad, Appl. Phys. A 90 (2008) 765–769.
[2] Q. Yang, J. Sha, X. Ma, D. Yang, Mater. Lett. 59 (2005) 1967–1970.
[3] Z.M. Jarzebski, Oxide Semiconductors, Pergamon Press, Poland, 1973.
[4] P. Puspharajah, S. Radhakrishna, A.K. Arof, J. Mater. Sci. 32 (1997) 3001–3006.
[5] A. Gupta, H.S. Bhatti, D. Kumar, N.K. Verma, R.P. Tandon, Digest J. Nanomater. Biostruct. 1 (2006) 1–9.
[6] U.S. Joshia, R. Takahashia, Y. Matsumotoa, H. Koinuma, Thin Solid Films 486 (2005) 214–217.
[7] H. Sato, T. Minami, S. Tanaka, T. Yamada, Thin Solid Films 236 (1993) 27.
[8] S.H. Lin, F.R. Chen, J.J. Kai, Appl. Surf. Sci. 254 (2008) 3357.
[9] Z. Zhu, N. Wei, H. Liu, Z. He, Adv. Powder Technol., doi:10.1016/j.apt.2010.06.008.
[10] X. Chen, Z. Zhang, C. Shi, X. Li, Mater. Lett. 62 (2008) 346–351.
[11] X. Ni, Q. Zhao, F. Zhou, H. Zheng, J. Cheng, B. Li, J. Cryst. Growth 289 (2006) 299–302.
[12] K.-T. Kim, G.-H. Kim, J.-C. Woo, C. Kim, Surf. Coat. Technol. 202 (2008) 5650–5653.
[13] A.A. Al-Ghamdi, E. Mahmoud Waleed, S.J. Yaghmour, F.M. Al-Marzouki, J. Alloy Compd. 486 (2009) 9–13.
[14] A. Berlich, Y.C. Liu, H. Morgner, Radiat. Phys. Chem. 74 (2005) 201–209.
[15] X.H. Huang, J.P. Tu, X.H. Xi, X.L. Wang, J.Y. Xiang, L. Zhang, Y. Zhou, J. Power Sources 188 (2009) 588–591.
[16] M.S. Niasari, N. Mir, F. Davar, Polyhedron 28 (2009) 1111–1114.
[17] C.S. Carney, C.J. Gump, A.W. Weimer, Mater. Sci. Eng. A 431 (2006) 1.
[18] B. Pandey, S. Ghosh, P. Srivastava, D.K. Avasthi, D. Kabiraj, J.C. Pivin, J. Magn. Mater. 320 (2008) 3347–3351.
[19] K. Ueda, H. Tabata, T. Kawai, Appl. Phys. Lett. 79 (2001) 988.
[20] R. Romero, F. Martin, J.R. Ramos-Barrado, D. Leinen, Thin Solid Films 518 (2010) 4499–4502.
[21] Y.R. Park, K.J. Kim, J. Cryst. Growth 258 (2003) 380–384.
[22] Y. Zuo, S. Ge, Z. Chen, L. Zhang, X. Zhou, S. Yan, J. Alloy Compd. 470 (2009) 47–50.
[23] S. Thota, L.M. Kukreja, J. Kumar, Thin Solid Films 517 (2008) 750–754.
[24] M. Caglar, J. Wub, K. Li, Y. Caglar, S. Ilican, D. Xue, Mater. Res. Bull. 45 (2010) 284–287.
[25] S. Ilican, Y. Caglar, M. Caglar, M. Kundakci, A. Ates, Int. J. Hydrogen Energy 34 (2009) 5201–5207.
[26] Y. Caglar, M. Caglar, S. Ilican, A. Ates, J. Phys. D: Appl. Phys. 42 (2009) 065421.
[27] Joint Committee on Powder Diffraction Standards (JCPDS), Powder Diffraction File, card no: 36-1451.
[28] Joint Committee on Powder Diffraction Standards (JCPDS), Powder Diffraction File, card no: 47-1049.
[29] B.D. Cullity, S.R. Stock, Elements of X-Ray Diffraction, 3rd ed., Prentice Hall, 2001.
[30] R.D. Shannon, Acta Cryst. A32 (1976) 751.